

# Prediction of Temperature and Contaminant Concentration Profiles in a Room with Impinging Jet Ventilation System by Zonal Model

Haruna Yamasawa<sup>\*1</sup>, Tomohiro Kobayashi<sup>2</sup>, Toshio Yamanaka<sup>2</sup>, Narae Choi<sup>2</sup>,  
Mathias Cehlin<sup>3</sup>, and Arman Ameen<sup>3</sup>

*1 Kyushu University  
6-1, Kasuga-koen, Kasuga-city  
Fukuoka, Japan*

*\*Corresponding and Presenting author:  
yamasawa@eee.kyushu-u.ac.jp*

*2 Osaka University  
2-1, Yamadaoka, Suita-city  
Osaka, Japan*

*3 University of Gävle  
SE-801 76  
Gävle, Sweden*

## ABSTRACT

The impinging jet ventilation (IJV) system has been proposed as a new air distribution strategy and is expected to overcome the disadvantages of the mixing ventilation system (MV), which is the most widely used system, and displacement ventilation, which provides better air quality than MV.

The present study aims to predict the temperature and contaminant distribution by a simple calculation model that is applicable for IJV with multiple heating elements inside the room. The present calculation model is based on the zonal model and turbulence jet theory. The concept and theory of the calculation model are introduced, and the calculation results are compared to that of CFD analysis.

The correlation between the thickness of the jet along the floor and the radial coordinate is obtained by the results of CFD analysis under isothermal conditions and adapted to the model as the height of the first zone from the floor. The turbulent diffusion coefficient of heat in the vertical direction is identified by the CFD results of the vertical temperature profile, whereas the turbulent diffusion coefficient of heat in the horizontal direction is obtained by the function of the number of heating elements in the present paper. It has to be noted that the turbulent diffusion coefficient of heat and contaminant is treated to be equal, due to the assumption in the present paper that the turbulent Prandtl number and the turbulent Schmidt number are the same.

Finally, the turbulent diffusion coefficient of vertical direction is expressed as the function of the Archimedes number (balance between buoyancy and inertial force of supply flow) defined in the present paper. The correlation was expressed by the equation from the previous study and also by the newly developed equation. It was shown that although some limitations exist, the calculation model developed in the present paper can predict the temperature and contaminant gradient in the room.

The calculation results of temperature gradient fitted that of CFD well except for the cases with large supply velocity. However, those cases are not practically applicable, thus, the accuracy of the model is more important in the cases with supply velocity lower than those cases. Although the calculation results of contaminant concentration fitted that of CFD analysis well in some cases, the prediction accuracy of contaminant concentration is generally lower than that of temperature. It is assumed to be because of the assumption in the present calculation model that the thermal and material turbulent diffusion coefficients are equal. Moreover, it is assumed that the modelling of the flow along the wall and the thermal plume from heating elements also need to be improved to increase the accuracy of the calculation model.

## KEYWORDS

Impinging Jet Ventilation, Zonal Model, Temperature Stratification, Contaminant Concentration, Diffusion Coefficient



## 2.1 Height of the zones

In the previous study [9], the CFD analysis was conducted to investigate the turbulent flow feature of IJV (especially about the width of jet along the floor) for the calculation model. Under the assumption that the jet width  $\delta$  [m] is the distance from wall where the velocity is smaller than a given value  $V_{limit}$  [m/s],  $\delta$  is expressed by the following equation:

$$\delta = 0.09 \frac{V_s}{V_m} D_s \left[ -\frac{1}{0.7} \log \left( \frac{V_{limit}}{V_m} \right) \right]^{1/2} \quad (1)$$

where,  $V_s$  is the supply velocity [m/s],  $V_m$  is the maximum velocity [m/s],  $D_s$  is the diameter of the supply duct [m], and  $b$  is half velocity width [m].  $V_m$  is set to be 0.5 m/s in the present paper by assuming that the impact of the jet is sufficiently small when  $V_m$  is smaller than 0.5 m/s. The ratio of  $V_{limit}$  to  $V_m$  mentioned prior is set to be 1% in the present paper so that it is considered to be possible to include more than 99% of the flow along floor by assuming the shape of flow feature to be a normal distribution.

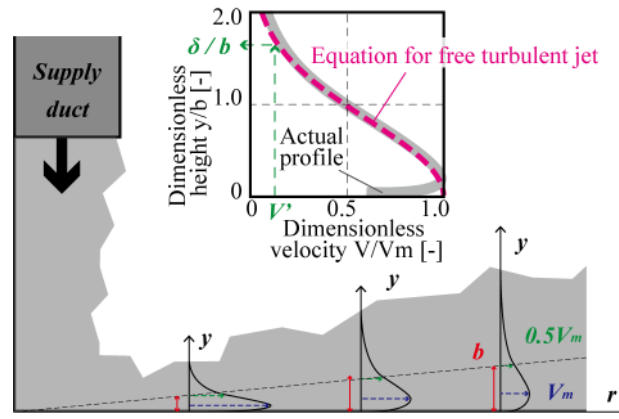


Figure 2: Concept of the calculation model

## 2.2 Wall-flow

The flow rate along heated or cooled walls (wall-flow) is studied by the previous studies and is adapted to the wall with temperature gradient as follows. The flow rate of the wall-flow is calculated by the equation below regarding the previous study [10]; and the temperature of the wall-flow,  $T_{wf}(j)$  [°C] is derived by Eq. (3), the method of Togari et al. [11] based on the boundary layer theory of turbulent jet [12].

$$\frac{\Delta F_{wf}(j)}{\Delta y} = 0.00330 \times |T_{ws}(j) - T_r(j)|^{2/5} \times y^{1/5} \times (\text{wall width}) \quad (2)$$

$$T_{wf}(j) = 0.25T_{ws}(j) + 0.75T_r(j) \quad (3)$$

The calculation procedure differs depending on the correlation between the temperatures of room ( $T_r$ ) air and wall surface ( $T_{ws}$ ) at each height. The case divisions for the wall-flow along the heated wall is illustrated in Figure 3. The situations are divided into three cases: when the temperature of wall surface is higher than that of the room both at the present height and zone above, the wall-flow keep moving upward; when the temperature of wall surface is higher than that of the room at the present height but the temperature of wall surface is equal to that of the room at the zone above, the wall-flow at the zone above does not exist and the wall-flow at the present height flows into the room zone above directly; and when the temperature of wall surface is higher than that of the room at the present height but the temperature of wall surface is lower than that of the room at the zone above, the wall-flow at the present height does not exist and the wall-flow from the zone below flow into the room zone at the present height directly. The calculation procedure for the cooled wall is the same as that of the heated wall.

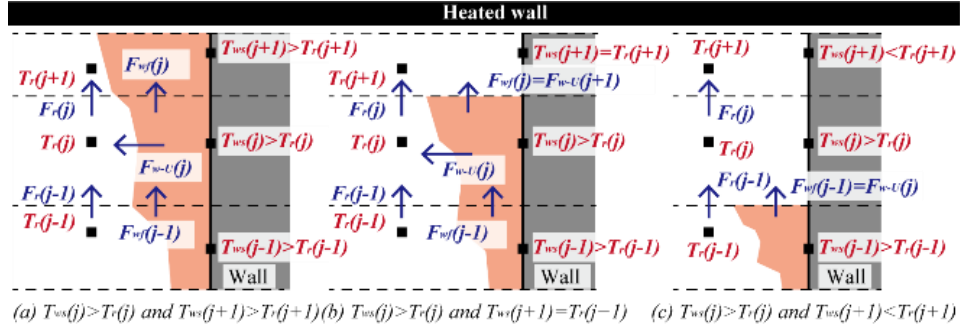


Figure 3: Concept of the calculation model

### 2.3 Thermal plume from heating element

At the height where heating elements exist, the flow rate and temperature of the plume is calculated by the same method as that of wall-flow (see Eq. (2) and Eq. (3)). On the other hand, at the height above the heating element, the flow rate of convection flow by cylinder is simulated by the method in the previous study [5,13]. Figure 4 illustrates the thermal plume above the heating element. The plume is simulated by a point heat source, and the flow rate was calculated by differentiating the equation in the previous study [5,13]. Where,  $T_{ref}$  is reference temperature [°C] ( $T_{ref} = 26$  °C),  $P_{HE}$  is heat generation rate from heating element [W], and  $D_p$  is diameter of the cylinder [m].

$$\frac{\Delta F_{pf}(y)}{\Delta y} = 31.7 \left[ \frac{g}{C_p \rho (T_{ref} + 273)} \right] P_{HE}^{\frac{1}{3}} \left[ y - \left\{ y_{p-H} - \frac{D_p}{2 \tan(12.5^\circ)} \right\} \right]^{\frac{2}{3}} \quad (4)$$

Temperature in the plume zone,  $T_{pf}(j)$  [°C], at the height above the heating element is derived by the conservation of heat at Zone-PF(j). Where,  $C_{b-h}$  is heat transfer coefficient by diffusion in the horizontal direction [W/m<sup>2</sup> K], which is to be explained later in section 2.7.

$$0 = C_p \rho [F_{pf}(j-1)T_{pf}(j-1) - F_{pf}(j)T_{pf}(j) - F_p(j)T_r(j)] + C_{b-h}S[T_r(j) - T_{pf}(j)] \quad (5)$$

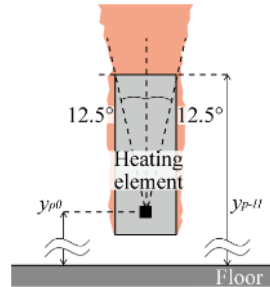


Figure 4: Concept of the calculation model

### 2.4 Mass conservation of air

Vertical airflow rate in the room zone,  $F_r(j)$  [m<sup>3</sup>/s], is derived by the mass conservation law at Zone-R(j) by assuming the density of air is constant. It has to be noted that  $F(0) = F_s$ .

$$0 = F_r(j-1) - F_r(j) + F_p(j) \times N_{HE} + \sum_{k=1}^{N_w} [F_w(j, k)] \quad (6)$$

### 2.5 Heat balance

Temperature in the room zone,  $T_r(j)$  [°C] is derived by the heat conservation law at Zone-R(j).

$$0 = \Delta Q_{r-c} + \Delta Q_{p-c} + \Delta Q_{w-c} + (\Delta Q_{r-d} + \Delta Q_{p-d} + \Delta Q_{w-d}) \quad (7)$$

The heat transfer by convection between room zones ( $\Delta Q_{r-c}$ ) [W], between room zone and plume zone ( $\Delta Q_{p-c}$ ) [W] and between room zone and wall-flow zone ( $\Delta Q_{w-c}$ ) [W] are expressed by equations as follows.

$$\Delta Q_{r-c} = C_p \rho F_r(j) [T_r(j+1) - T_r(j)] - C_p \rho F_r(j-1) [T_r(j-1) - T_r(j)] \quad (8)$$

$$\Delta Q_{p-c} = C_p \rho F_p(j) [T_p(j-1) - T_r(j)] \quad (9)$$

$$\Delta Q_{w-c} = C_p \rho \sum_{k=1}^{N_w} \{F_{w-U}(j, k) [T_{wf}(j-1, k) - T_r(j)] + F_{w-L}(j, k) [T_{wf}(j+1, k) - T_r(j)]\} \quad (10)$$

Due to the conservation of mass, the total flow rate of outflow from Zone-R(j) is equal to that of inflow. Therefore, within Eq. (8) to Eq. (10), the terms that include the flow rate with the flow direction of outflow should be ignored. It has to be noted that  $T_r(0) = T_s$  and  $F_r(0) = F_s$  are substituted during the calculation. The heat transfer by diffusion between room zones ( $\Delta Q_{r-d}$ ) [W], between room zone and plume zone ( $\Delta Q_{p-d}$ ) [W] and between room zone and wall-flow zone ( $\Delta Q_{w-d}$ ) [W] are expressed by equations as follows.

$$\Delta Q_{r-d} = C_{b-v} S [T_r(j+1) - T_r(j)] + C_{b-v} S [T_r(j-1) - T_r(j)] \quad (11)$$

$$\Delta Q_{w-d} = \sum_{k=1}^{N_w} \{C_{b-h} S [T_{ws}(j, k) - T_r(j)]\} \quad (12)$$

$$\Delta Q_{p-d} = C_{b-h} S [T_{pf}(j) - T_r(j)] \quad (13)$$

$$C_{b-v} = \frac{C_p \rho a_{t-v}}{L} \quad (14)$$

where,  $C_{b-v}$  is heat transfer coefficient by diffusion in the vertical direction [W/m<sup>2</sup> K],  $a_{t-v}$  is turbulent diffusion coefficient in the vertical direction [m<sup>2</sup>/s], and  $L$  is the distance between the centre of zones [m].

## 2.6 Mass conservation of contaminant

The contaminant was treated as a passive contaminant, and its conservation is solved by almost the same procedure as that of the heat balance. Each term in Eq. (15) except for  $M_p$  [m<sup>3</sup>/s] corresponds to Eq. (8) to Eq. (14) in the calculation of heat balance and can be obtained by changing the temperature in those equations to the contaminant and divide them by volumetric heat capacity,  $C_p \rho$  [J/m<sup>3</sup>K]. The contaminant concentration in the room zone,  $C_r(j)$  [-], is derived by the mass conservation law of contaminant at Zone-R(j).

$$0 = \Delta M_{r-c} + \Delta M_{p-c} + \Delta M_{w-c} + (\Delta M_{r-d} + \Delta M_{p-d} + \Delta M_{w-d}) + M_p \quad (15)$$

$$C_{c-v} = \frac{C_{b-v}}{C_p \rho} = \frac{a_{t-v}}{L} \quad (16)$$

where,  $M_p$  is the emission of contaminant [m<sup>3</sup>/s], and  $C_{c-v}$  is material transfer coefficient by diffusion [m/s]. Eq. (16) means that the turbulent diffusion coefficient of heat and contaminant are treated to be the equal, due to the assumption in the present paper that the turbulent Prandtl number and the turbulent Schmidt number are the same.

## 2.7 Modelling of diffusion flux

Togari et al. [11] adopted a fixed value for the turbulent heat transfer coefficient in vertical direction,  $C_{b-v}$  [W/m<sup>2</sup> K], whereas Kobayashi et al. [14] identified the value of turbulent thermal diffusivity in vertical direction,  $a_{t-v}$  [m<sup>2</sup>/s], by the CFD result. In the present paper,  $a_{t-v}$  is to be identified based on the results of CFD analysis in the previous study [15] later in section 3. To clarify the balance between buoyancy and inertial force in each case, Kobayashi et al. [14] adopted Archimedes number, and expressed the correlation between Archimedes number and identified  $a_{t-v}$ . The following Archimedes number  $Ar_{room}$  [-] [16,17] was defined and adopted in the present paper:

$$Ar_{room} = \frac{g \beta H_c (T_e - T_s)}{V_s^2} \quad (17)$$

where  $g$  is gravity acceleration [m/s<sup>2</sup>],  $\beta$  is thermal expansion coefficient [1/K],  $H_c$  is height of room [m], and  $V_s$  is supply velocity [m/s]. According to Kobayashi et al. [14], the correlation between  $a_{t-v}$  and  $Ar_{room}$  is to be expressed by Eq. (18), where  $\eta$  is coefficient. However, to improve the prediction accuracy of the calculation model, the correlation is also expressed by Eq. (19) in the present paper.

$$a_{t-v} = \eta_1 \times Ar_{room}^{-\eta_2} \quad (18)$$

$$a_{t-v} = \eta_2 - \eta_3 [1 - \exp(\eta_4 \times Ar_{room})] \quad (19)$$

Turbulent heat transfer coefficient in horizontal direction,  $C_{b-h}$ , is given by a constant value in previous studies; Kobayashi et al. [14] adopted  $C_{b-h} = 1.0$  [W/m<sup>2</sup> K]. However, according to the results of previous numerical investigation [15], horizontal contaminant concentration showed more uniform distribution at the cases with higher occupant density. It was because that the convection current above the heating elements easily be merged when the heating elements were close to each other. Thus, it is assumed that the occupant density can be a parameter to explain this difference. Therefore, in the present model,  $C_{b-h}$  is to be expressed as the function of occupant density, and assumed to be in proportion to the “coverage ratio ( $S_{HE-h} \times N_{HE}/S_{r-h} = S_{HE-h} \times (occupant\ density)$ )” of the heating elements as follows.

$$C_{b-h} = \eta_5 \frac{S_{HE-h} \times N_{HE}}{S_{r-h}} \quad (20)$$

where,  $\eta_3$  is model coefficient [-],  $S_{HE-h}$  and  $S_{r-h}$  are the area of the horizontal cross-section of each heating element and room [m<sup>2</sup>], respectively, and  $N_{HE}$  is the number of the heating element.

The coefficients in the present section are obtained using the least-squares method by comparing the vertical temperature profiles predicted by CFD analysis and the zonal model.

### 3 VALIDATION OF CALCULATION MODEL BY CFD

#### 3.1 Methodology

To validate the calculation model, part of the numerical results in the previous study [15] is to be compared to that of the calculation model. The geometrical configuration and studied cases are summarised in Figure 5, and the studied cases and inlet velocity are summarised in Table 1. As the boundary conditions,  $k = 0.2$  m<sup>2</sup>s<sup>-2</sup> and  $\omega = 4.7$  s<sup>-1</sup> are adopted at the inlet boundary; the standard heat transfer coefficient (2.27 – 4.69 W/m<sup>2</sup>K) and the external temperature of 28.0 °C are adopted at each wall. The CFD analysis was conducted using Ansys Fluent 19.2 with the turbulence model of SST  $k-\omega$  model, and the discretization scheme for advection was QUICK. The radiation was calculated by the Surface-to-surface model, and internal emissivity of 0.85 was adopted for the walls. The geometry of the heating elements was set to be 0.4 × 0.4 × 1.0 m and located 0.4 m above the floor, assuming seated occupants with a sensible heat generation rate of 60 W per person. The contaminant was released above the human simulators as the tracer of the bioeffluents from the human body. The contaminant was emitted as the passive contaminant by a rate of 1.0 × 10<sup>-5</sup> kg/m<sup>3</sup> s. As for the calculation model, the contaminant was emitted at the same height as that at CFD analysis, 1.4 to 1.5 m above the floor, within the plume flow above the occupants.

The parameters are the number of heating elements (9, 16, 25 and 36), i.e., occupant density (0.11, 0.20, 0.31 and 0.44), and supply duct (1, 2, 4 and 6), i.e., sixteen cases were studied in total. The bottom of the supply duct was mounted 0.6 m above the floor, and the exhaust opening was located in the middle of the ceiling. Both supply duct and exhaust opening have an area of 0.3 × 0.3 m = 0.09 m<sup>2</sup>. The supply flow rate was set to be 60 m<sup>3</sup>/h per person, and the supply temperature was 23 °C. The supply velocity was differed from 0.278 – 6.67 m/s depending on the number of occupants and the number of supply ducts.

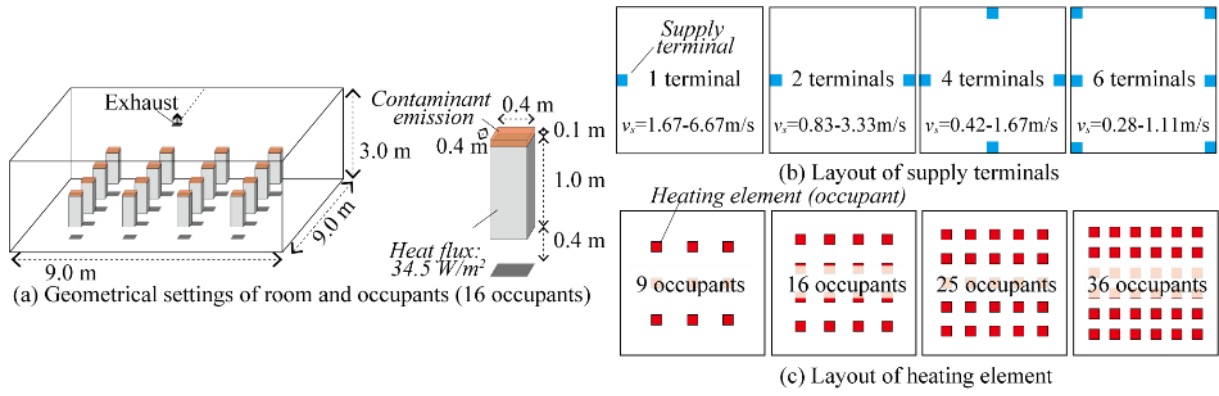


Figure 5: Concept of the calculation model

Table 1 Supply and exhaust velocity at studied cases

	$N_{HE} = 9$ occupants Occupant density: 0.11 ( $F_s = 540 \text{ m}^3/\text{h}$ )	$N_{HE} = 16$ occupants Occupant density: 0.20 ( $F_s = 960 \text{ m}^3/\text{h}$ )	$N_{HE} = 25$ occupants Occupant density: 0.31 ( $F_s = 1,500 \text{ m}^3/\text{h}$ )	$N_{HE} = 36$ occupants Occupant density: 0.44 ( $F_s = 2,160 \text{ m}^3/\text{h}$ )
Exhaust	1.67 m/s	2.96 m/s	4.63 m/s	6.67 m/s
1 terminal	1.67 m/s	2.96 m/s	4.63 m/s	6.67 m/s
2 terminals	0.833 m/s	1.48 m/s	2.31 m/s	3.33 m/s
4 terminals	0.417 m/s	0.741 m/s	1.16 m/s	1.67 m/s
6 terminals	0.278 m/s	0.494 m/s	0.772 m/s	1.11 m/s

### 3.2 Results and discussion

The vertical profiles of temperature and contaminant concentration obtained by CFD and calculation model are shown in Figure 6. The concentration is shown by the normalized form (concentration at each height / exhaust concentration). The results of CFD analysis and calculation were compared at the case with sixteen occupants and four supply terminals as a standard case, and  $\eta_5$  in Eq. (20) was calculated to be approximately 800 by the least-squares method with one significant digit.

The numerical result is shown by grey line and the result of calculation with identified  $a_{t-v}$  is shown by red line in Figure 6. The correlation between  $Ar_{room}$  and the identified results of  $a_{t-v}$  are summarised in Figure 7. Using Eq. (18) and Eq. (19), the correlation between  $Ar_{room}$  [-] and  $a_{t-v}$  [ $\text{m}^2/\text{s}$ ] is shown by the equations below.

$$a_{t-v} = 0.00570 \times Ar_{room}^{-0.569} \quad (21)$$

$$a_{t-v} = 0.169 - 0.163[1 - \exp(30.0 \times Ar_{room})] \quad (22)$$

The calculation was also conducted with  $a_{t-v}$  predicted by Eq. (21) and Eq. (22), and the results are also shown in Figure 6 by blue and purple broken lines.

In general, the calculation results with identified  $a_{t-v}$  fits the CFD results well. Especially, when comparing the numerical and calculated results of temperature. However, when comparing the temperature profiles of the cases with  $V_s \geq 2.96 \text{ m/s}$  or  $Ar_{room} \leq 4.65 \times 10^{-2}$ , the prediction accuracy of calculation model is not as high as the other cases. It is assumed to be because of the assumption of the model; the assumption that the temperature stratification exists in the room under the cooling operation by IJV. Therefore, for the cases under mixed condition, the prediction accuracy is not as high as the cases with temperature stratification. However, since temperature stratification is essential for IJV to achieve high ventilation effectiveness, the low accuracy in the cases without stratification is assumed to be merely a minor drawback, and negligible for the use of the calculation model.

Although the calculation of temperature by the model has a high prediction accuracy in general, the calculation results (red and blue lines) of contaminant are different from that of CFD (grey line) when occupant density is high. The major reason for this is assumed to be because the thermal and material turbulent diffusion coefficients are set to be equal in the

present paper. It means that the turbulent Prandtl number and turbulent Schmidt number should not have been treated as equal.

When comparing the calculated results with identified  $a_{t-v}$  (red line) and predicted  $a_{t-v}$  (blue line and purple line), the results of the temperature were almost the same. When comparing the results of blue and purple lines, the prediction accuracy is higher for the purple line than that for blue line, i.e., Eq. (19) has better prediction accuracy than that of Eq. (18).

In addition, to understand the validity of the non-constant value of  $C_{b-h}$  on the indoor environment, the calculation results with constant  $C_{b-h}$  ( $C_{b-h} = 1.0 \text{ W/m}^2\text{K}$ ) is also shown in Figure 6 by green lines. As for  $a_{t-v}$ , the same value with the red lines is adopted. In Figure 6, it was shown that the calculated results of temperature with  $C_{b-h} = 1.0$  are lower than those of other results, especially when the occupant density is high. Thus, the assumption that “the diffusion of horizontal direction is affected by the occupant density” is assumed to be appropriate. However, the most proper way to correlate the occupant density and  $C_{b-h}$  is not yet fully investigated.

It was shown that the temperature and contaminant gradient in the room can be roughly predicted by the present calculation model. However, there are still some limitations, i.e., the prediction accuracy of contaminant distribution by the calculation model is not as high as that of temperature. Although the mentioned limitations still exist, it was shown that the calculation model can predict the temperature and contaminant concentration gradient in a room with IJV depending on the design conditions.

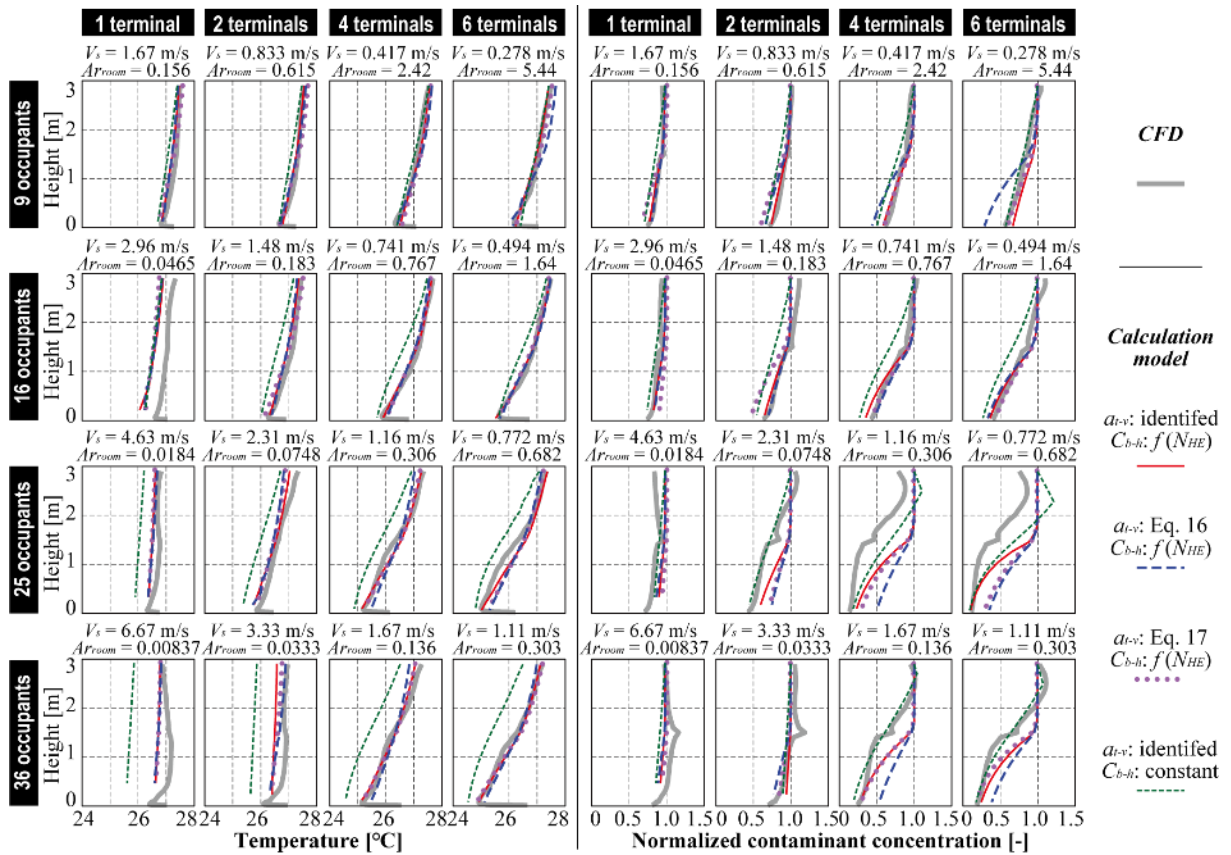


Figure 6: Concept of the calculation model

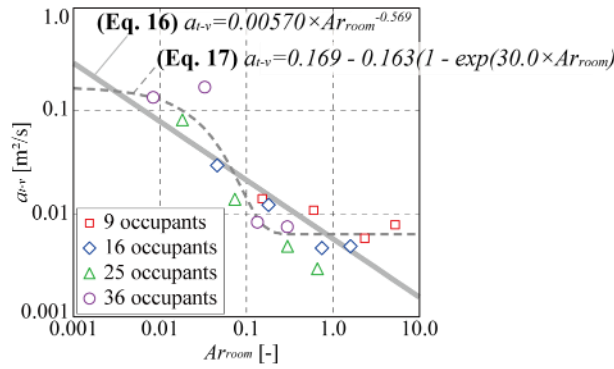


Figure 7: Concept of the calculation model

## 4 CONCLUSIONS

Using turbulent jet theory, the method for predicting the vertical profile of temperature and contaminant concentration in a room with IJV is developed in the present paper. The balance between supply momentum and buoyancy are expressed by Archimedes number,  $Ar_{room}$ , and the vertical turbulent diffusion coefficient in the calculation model is finally expressed as the function of  $Ar_{room}$ . On the other hand, the horizontal turbulent diffusion coefficient was expressed as the function of the occupant density. The present work is believed to enhance the designer to predict the indoor environment of a room with IJV during the design phase. The findings are summarised as follows:

- The calculation results of temperature gradient fitted that of CFD well except for the cases with large supply velocity, i.e., larger than 2.96 m/s. However, those cases are not practically applicable, thus, the accuracy of the model is more important at the cases with supply velocity lower than those cases.
- Although the calculation results of contaminant concentration fitted that of CFD well in some cases, the prediction accuracy of contaminant concentration is generally lower than that of temperature. It is assumed to be because of the assumption in the present calculation model that the thermal and material turbulent diffusion coefficients are equal.
- It was shown that the calculated results with identified and predicted turbulent diffusion coefficient are almost the same in temperature gradient. In addition, the newly developed equation for expressing the correlation between the turbulent diffusion coefficient and the Archimedes number could improve the prediction accuracy.
- The calculation results of both temperature and contaminant concentration have improved by expressing the turbulent diffusion coefficient in horizontal direction as the function of the occupant density. However, the suitable way of expressing the coefficient is still needed to be investigated.

## 5 ACKNOWLEDGEMENTS

A part of this work was supported by JSPS KAKENHI Grant Number JP20J10608 (Principal Investigator, Haruna Yamasawa).

## 6 REFERENCES

- [1] European Commission, The European Green Deal, Eur. Comm. (2019) 1–24. <https://eur-lex.europa.eu/legal-content/EN/TXT/PDF/?uri=CELEX:52019DC0640&from=EN>.
- [2] Ministry of Economy Trade and Industry of Japan, Annual report on energy (in Japanese), 2020. <https://www.enecho.meti.go.jp/about/whitepaper/2020pdf/>.

- [3] Ministry of the Environment of Sweden, Sweden submits long-term climate strategy to UN, Gov. Off. Sweden. (2020). <https://www.government.se/press-releases/2020/12/sweden-submits-long-term-climate-strategy-to-un/> (accessed July 16, 2021).
- [4] M. Sandberg, C. Blomqvist, Displacement ventilation systems in office rooms, *ASHRAE Trans.* 95 (1989) 1041–1049.
- [5] R. Kosonen, A. Melikov, E. Mundt, P. Mustakallio, P. V Nielsen, Displacement Ventilation, *Rehva Guidebook No. 23*, REHVA, Brussels, 2002.
- [6] T. Karimipanah, M. Sandberg, H.B. Awbi, A Comparative Study of Different Air Distribution Systems in a Classroom, in: *Roomvent*, Reading, 2000: pp. 1013–1018.
- [7] T. Karimipanah, H.B. Awbi, Theoretical and experimental investigation of impinging jet ventilation and comparison with wall displacement ventilation, *Build. Environ.* 37 (2002) 1329–1342. [https://doi.org/10.1016/S0360-1323\(01\)00117-2](https://doi.org/10.1016/S0360-1323(01)00117-2).
- [8] H. Yamasawa, T. Kobayashi, T. Yamanaka, N. Choi, M. Cehlin, A. Ameen, Prediction of thermal and contaminant environment in a room with impinging jet ventilation system by zonal model, *Build. Environ.* 221 (2022) 109298. <https://doi.org/10.1016/j.buildenv.2022.109298>.
- [9] H. Yamasawa, T. Kobayashi, T. Yamanaka, N. Choi, M. Cehlin, A. Ameen, Prediction of thermal and contaminant environment in a room with impinging jet ventilation system by zonal model, *Build. Environ.* 221 (2022) 109298. <https://doi.org/10.1016/j.buildenv.2022.109298>.
- [10] T. Yamanaka, H. Kotani, M. Xu, Zonal Models to Predict Vertical Contaminant Distribution in Room with Displacement Ventilation Accounting for Convection Flows along Walls, in: *IAQVEC 2007 Proc. - 6th Int. Conf. Indoor Air Qual. Vent. Energy Conserv. Build. Sustain. Built Environ.*, 2007.
- [11] S. Togari, Y. Arai, K. Miura, A simplified model for predicting vertical temperature distribution in a large space, *ASHRAE Trans.* 99 (1993) 84–99.
- [12] E.R. Eckert, T.W. Jackson, Analysis of Turbulent Free-Convection Boundary Layer on Flat Plate, (1950). <https://apps.dtic.mil/sti/citations/ADA382013>.
- [13] H. Skistad, *Displacement Ventilation*, Research Studies Press Ltd., 1994.
- [14] T. Kobayashi, N. Umemiya, Simplified prediction using block model for vertical profile of temperature and contaminant concentration in a room with impinging jet ventilation, *Build. Environ.* 209 (2021) 108643. <https://doi.org/10.1016/j.buildenv.2021.108643>.
- [15] H. Yamasawa, T. Kobayashi, T. Yamanaka, N. Choi, M. Cehlin, A. Ameen, Effect of supply velocity and heat generation density on cooling and ventilation effectiveness in room with impinging jet ventilation system, *Build. Environ.* 205 (2021) 108299. <https://doi.org/10.1016/j.buildenv.2021.108299>.
- [16] H. Yamasawa, T. Kobayashi, T. Yamanaka, N. Choi, M. Matsuzaki, Experimental investigation of difference in indoor environment using impinging jet ventilation and displacement ventilation systems, *Int. J. Vent.* (2021) 1–18. <https://doi.org/10.1080/14733315.2020.1864572>.
- [17] H. Yamasawa, T. Kobayashi, T. Yamanaka, N. Choi, M. Cehlin, A. Ameen, Applicability of displacement ventilation and impinging jet ventilation system to heating operation, *Japan Archit. Rev.* 4 (2021) 403–416. <https://doi.org/10.1002/2475-8876.12220>.